

Recoupled Polarization Transfer Heteronuclear ^1H – ^{13}C Multiple-Quantum Correlation in Solids under Ultra-fast MAS

Kay Saalwächter, Robert Graf, and Hans W. Spiess¹

Max-Planck-Institute for Polymer Research, Postfach 3148, D-55021 Mainz, Germany

Received April 2, 1999; revised June 10, 1999

A new approach for high-resolution solid-state heteronuclear multiple-quantum MAS NMR spectroscopy of dipolar-coupled spin- $\frac{1}{2}$ nuclei is introduced. The method is a heteronuclear chemical shift correlation technique of abundant spins, like ^1H with rare spins, like ^{13}C in natural abundance. High resolution is provided by ultra-fast MAS and high magnetic fields, high sensitivity being ensured by a direct polarization transfer from the abundant protons to ^{13}C . In a rotor-synchronized variant, the method can be used to probe heteronuclear through-space proximities, while the heteronuclear dipolar coupling constant can quantitatively be determined by measuring multiple-quantum spinning-sideband patterns. By means of recoupling, even weak heteronuclear dipolar interactions are accessible. The capabilities of the technique are demonstrated by measurements on crystalline L-tyrosine hydrochloride salt. © 1999 Academic Press

Key Words: multiple-quantum spectroscopy; heteronuclear dipolar correlation; recoupling methods; spinning-sideband patterns; magic-angle spinning.

The use of two-spin modes such as homonuclear double-quantum coherences has been shown to be a versatile approach in solid-state NMR spectroscopy for the determination of molecular parameters such as internuclear distances (I) and torsion angles (2, 3). Even the structural elucidation of complex hydrogen-bonded systems has become possible (4). However, in the case of abundant proton systems, homonuclear ^1H – ^1H double-quantum techniques are limited by a lack of spectral resolution, even at the highest magic-angle spinning (MAS) speeds available. By taking advantage of the larger spread of chemical shifts of rare spins, such as ^{13}C , the amount of information which can be harnessed from double- and multiple-quantum (MQ) spectra is greatly increased (5, 6).

In this paper, we introduce a novel high-resolution solid-state NMR technique employing heteronuclear multiple-quantum coherences to abundant spins. The experiment is termed recoupled polarization transfer–heteronuclear multiple-quantum correlation (REPT-HMQC) and employs heteronuclear dipolar couplings to excite multiple-quantum coherences. The pulse sequence can be used either to correlate ^{13}C – ^1H chemical shifts in a two-dimensional experiment or to evaluate dipolar

coupling constants in a quantitative manner by measuring multiple-quantum spinning sideband patterns. Furthermore, spectral editing can be accomplished by measuring one-dimensional HMQ-filtered spectra. Thus, the advantages of high-speed spinning can be exploited in ^{13}C NMR.

Heteronuclear correlation (HETCOR) techniques are among the most important methods for advanced structural elucidation. In the solid state, such techniques have proven useful to achieve ^1H wideline separation (WISE-NMR, (7)) to study the dynamics in complex polymer systems, in spectral editing (8, 9), and for obtaining distance constraints (10). We present here a method which combines the advantages of multiple-quantum NMR and the wealth of information obtainable from HETCOR experiments. Previous work has concentrated on the quasistatic excitation of heteronuclear double-quantum coherences (6) which were excited using synchronous irradiation on both channels. However, since this method is limited to excitation times of half a rotor period and thus to strongly dipolar-coupled spins like directly bound ^1H – ^{13}C pairs at moderate spinning frequencies, it is obviously desirable to extend the method so that it is applicable to weaker couplings at very high MAS frequencies—the latter being necessary to simplify the dipolar coupling amongst the abundant spins (11), leading to optimum resolution in the MQ dimension and hence spectral simplification.

To this end, a robust recoupling method for the selective excitation of heteronuclear MQ coherences has been developed. The pulse scheme for our experiment is depicted in Fig. 1. Considering only the five 90° pulses following the saturation pulse comb on the S spin channel and the refocusing π -pulse in t_1 , the pulse sequence corresponds to an HMQC experiment involving a polarization transfer from protons to carbons. This polarization transfer renders the sequence applicable to samples naturally abundant in ^{13}C , since one benefits from the high initial polarization and the short T_1 relaxation time of protons. The experiment was first applied in solution-state NMR and dates back to the first publication of the HMQC idea (12). The HMQC experiment, as popularized by Bax in the early 1980s (13), was designed to yield information on heteronuclear correlations in solution-state NMR and utilized the scalar J coupling between protons and rare spin species such as ^{13}C or ^{15}N .

¹ To whom correspondence should be addressed.

An extension of this technique to perform high resolution HETCOR experiments through J couplings in solids has recently been reported (9), the method being termed MAS-J-HMQC by the authors.

Before discussing the application to solid-state NMR, we shall in short outline the basic stages of the experiment. The proton transverse magnetization created by the first 90° pulse evolves into antiphase magnetization $I_x S_z$ under the action of heteronuclear *dipolar* or scalar couplings. The second 90° pulse converts the antiphase magnetization into a term proportional to

$$I_x S_x = \frac{1}{4}(I_+ S_+ - I_- S_-) + \frac{1}{4}(I_+ S_- - I_- S_+), \quad [1]$$

which constitutes a mixture of 2-spin zero- and double-quantum coherences. This coherence state then evolves during t_1 under the chemical shift interaction of the two nuclei involved and (dipolar) couplings to additional spins. The π -pulse in the middle of the t_1 evolution period refocuses all heteronuclear couplings of the S spin and its isotropic chemical shift, leaving the proton chemical shift as the defining interaction in t_1 . Additionally, the π -pulse interchanges zero- and double-quantum coherences; thus the refocused sequence is only capable of detecting the above mixture of both types of coherence. Dipolar couplings of the involved two spins to other spins lead to line broadening in F_1 and deviations from the expected spinning sideband patterns. After applying another 90° pulse to the

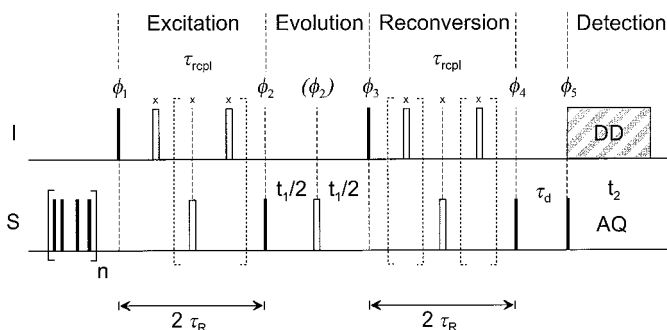


FIG. 1. Pulse sequence for the two-dimensional REPT-HMQC experiment. Narrow black bars correspond to 90° pulses and open bars represent 180° pulses. In order to avoid interference from directly excited ^{13}C signals, a saturation pulse train is applied to the S spin channel prior to the experiment. The MQ excitation and recoupling periods are made up of REDOR π -pulse trains. The scheme depicted here represents fully offset—and for ^{13}C chemical shift anisotropy compensated—recoupling periods of duration $2\tau_R$. For just one rotor period of recoupling, two π -pulses in each period (dotted brackets) and the corresponding delays are omitted. For higher recoupling times, π -pulses on the proton channel have to be repeated with $0.5\tau_R$ spacings and may be cycled according to the XY-4 phase cycling scheme (26) to render the pulse train insensitive to spectral offsets. The phases of the REDOR pulses are kept constant during the whole experiment, with the phases of the five HMQC pulses being listed in Table 1. To achieve sign-sensitive detection in t_1 , the TPPI method (27) can be implemented by incrementing the phase of the reconversion pulse ϕ_3 by 90° for subsequent slices in t_1 .

TABLE 1
Proposed Phase Cycle for the REPT-HMQC Pulse Sequence

ϕ_1	$xyy\bar{x}\bar{y}\bar{y}$
ϕ_2	$y\bar{y}\bar{x}\bar{y}yx\bar{x}$
ϕ_3	$yy\bar{x}\bar{y}yx$
ϕ_4	$\bar{x}\bar{y}yxxy$
ϕ_5	$y\bar{y}\bar{x}\bar{y}\bar{x}\bar{y}\bar{y}\bar{x}\bar{y}yx\bar{x}$
ϕ_{rec}^a	$xyy\bar{x}\bar{y}\bar{y}\bar{x}\bar{y}yx\bar{y}$

^a For the case $\tau_{rcpl} = 1\tau_R$, y and \bar{y} have to be interchanged.

I spins, the resulting S spin antiphase magnetization $I_z S_x$ evolves into observable S spin transverse magnetization, which is then subjected to a z filter (last pair of 90° pulses on the S spins) of duration τ_d in order to suppress unwanted signal contributions.

Under fast MAS, all dipolar couplings are significantly reduced and pair correlations prevail (11). Recoupling of the heteronuclear dipolar interaction can be achieved by applying a simple π -pulse train with half rotor periods spacings on either one of the two involved spin species. This method is termed rotational-echo double-resonance (REDOR) and has already found a great variety of applications (14–16). The π -pulse train not only recouples the dipolar interaction, but also refocuses the sample orientation independent heteronuclear scalar couplings; this interaction is thus neglected in the analytical treatment of the pulse sequence presented below. Also, all isotropic chemical shifts are refocused by the π -pulses, and during reconversion the single S spin π -pulse even corrects for any contribution of S spin chemical shift anisotropy (CSA), leaving the dipolar coupling under MAS as the only interaction to be considered during the recoupling periods of the experiment. It should be noted that a similar pulse sequence has been used previously to excite HMQ coherences between rare spins in an experiment to determine torsion angles in ^{13}C , ^{15}N doubly labeled amino acids (17). There, the orientation-dependent dipolar couplings of the ^{13}C – ^{15}N HMQ coherences to ^1H were evaluated in a separated local field experiment.

The average dipolar Hamiltonian under MAS for a REDOR π -pulse train in the secular approximation equals (15)

$$\bar{H}_{D,IS} = 2I_z S_z \bar{d}^{IS}(t), \quad [2]$$

where

$$\bar{d}^{IS}(t) = -\frac{D^{IS}}{2\pi} (2\sqrt{2} \sin 2\beta \sin(\omega_R t + \gamma)), \quad [3]$$

with ω_R denoting the angular spinning frequency. The angles β and γ correspond to the angle of the internuclear axis with respect to the rotor axis and the initial rotor phase, respectively. The dipolar coupling constant is given by

$$D^{IS} = \frac{\mu_0 \hbar}{4\pi} \frac{\gamma_I \gamma_S}{r_{IS}^3}, \quad [4]$$

Using the average dipolar Hamiltonian (Eq. [2]) for both the excitation and the recoupling periods of the experiment and neglecting contributions from S spin CSA during t_1 , straightforward product operator algebra (18) leads to the following expressions for the S -detected time domain signals in t_1 for an isolated IS spin pair,

$$S_x^S(t_1) \propto \langle \frac{1}{2} \sin(N\tau_R \bar{d}^{IS}(0)) \sin(N\tau_R \bar{d}^{IS}(t_1)) \cos(\omega_{CS,I} t_1) \rangle \quad [5]$$

$$S_y^S(t_1) \propto \langle \frac{1}{2} \sin(N\tau_R \bar{d}^{IS}(0)) \sin(N\tau_R \bar{d}^{IS}(t_1)) \sin(\omega_{CS,I} t_1) \rangle, \quad [6]$$

where $\langle \dots \rangle$ denotes the powder average to be taken over all orientations (β , γ). The two-dimensional experiment can be performed in two ways: Since the time-dependent dipolar coupling element $\bar{d}^{IS}(t)$ (Eq. [3]) is periodic with respect to one rotor period, $\tau_R = 2\pi/\omega_R$, it is obvious from the above equations that incrementing t_1 in steps of full rotor cycles leaves only the modulation of the t_1 signal with respect to the isotropic chemical shift $\omega_{CS,I}$ of the I spins. Thus a HETCOR spectrum is recorded in which the intensity of the crosspeaks is determined by the heteronuclear dipolar coupling and the number of recoupling cycles N . The first slice of the 2D data set after one Fourier transformation for $t_1 = 0$ represents a HMQ-filtered S spin spectrum. Incrementing t_1 in smaller steps gives a full MQ spinning sideband pattern in the t_1 dimension. The origin of these MQ spinning sidebands has been found to be the rotor encoding of the orientation-dependent dipolar Hamiltonian during the reconversion period (1, 19). From these spinning sidebands, the dipolar coupling constant and thus the internuclear distance can be derived. The spinning sideband pattern for the case of an isolated IS spin pair consists only of odd order sidebands; via the dependences in Eqs. [5], [6], the overall pattern is also dependent on the number of recoupling cycles N . In the case of very weak couplings and low values of N , only first order sidebands are visible, and the buildup of MQ intensity can be studied by increasing the recoupling time.

We demonstrate here the capabilities of the technique at the highest MAS rotor frequencies currently available by showing measurements of crystalline L-tyrosine hydrochloride salt on different spectrometers with proton resonance frequencies of 300 and 700 MHz. In Fig. 2, spectra recorded with $\tau_{repl} = \tau_R$ and $\tau_{repl} = 2\tau_R$ at 30 kHz MAS are compared for the two different magnetic field strengths. Clearly, the resolution in the proton (MQ) dimension is significantly increased at the higher magnetic field. The effect of higher magnetic fields on the proton resolution has been observed before in CP/WISE heteronuclear correlation spectra of L-tyrosine · HCl (10) and has

been explained by both the larger chemical shift frequency dispersion of protons in higher field and a more effective truncation of the strong dipolar couplings among the protons by the increased Zeeman interaction. Proton linewidths on the order of 1 ppm for abundant ^1H systems have only been observed before at high spinning frequencies (about 15 kHz) in HETCOR experiments using elaborate line narrowing techniques in the proton dimension, such as frequency switched Lee–Goldburg (FSLG) decoupling (9, 20) or in homonuclear single- and double-quantum spectra, using multiple-pulse irradiation (21, 22). It should be emphasized that all these techniques are very sensitive to effects of B_1 inhomogeneity and are strongly dependent on very precise settings of pulse durations and phases and on an exact rotor synchronization. The REPT-HMQC sequence in turn is rather robust, requiring no elaborate setup of the spectrometer or exact matching conditions, and only the approximate pulse lengths on both channels have to be determined. Spinning speed variations as large as ± 15 Hz at 30kHz MAS can be tolerated.

The assignment of proton and carbon signals in L-tyrosine · HCl has also been discussed before in great detail (20). The correlations visible for 1 τ_R recoupling time (Fig. 2, spectrum II) are one-bond correlations only; the information content compares well to that obtained from MAS-J-HMQC spectra. For 2 τ_R recoupling time, couplings of protons to quaternary carbons become visible. This is similar to the situation in the FSLG decoupled CP/WISE spectra, where even at short CP contact times of 100 μs these correlations are already visible. Here, visible correlations correspond to localized 2-spin modes, with perturbing effects like spin diffusion being excluded. Hence, each crosspeak corresponds to a well-defined dipolar-coupled ^1H – ^{13}C pair. As in the CP/WISE correlation spectra, even intermolecular couplings (e.g., the one of C_9 to the COOH proton, see arrow in spectrum IV) can be identified. An alternative explanation of these long-range crosspeaks in terms of relayed coherence transfer is unlikely for a sample at natural abundance and, in particular, when the substantial reduction of the homonuclear dipolar couplings by the very fast MAS is considered.

A very interesting feature visible in such highly resolved HETCOR spectra of L-tyrosine has obviously not yet been discussed: The chemical shift of the protons associated with C_5 and C_7 (and with C_6 and C_8 alike) is different by about 2 ppm, although as to their magnetic properties both positions should be equivalent on a molecular level. Clearly, a packing effect is observed here. We attribute the significant upfield shift on the proton at C_5 (and C_8) to the influence of the phenyl ring current in adjacent molecules in the crystal. Just recently in our group, similar effects have been observed in substituted hexabenzocoronene samples, disk-shaped molecules which are known to form columnar stacks in the solid phase (23). To our knowledge, such effects have not been reported before to be present in solid-state ^1H NMR spectra.

A limitation of the technique is obvious from the disappear-

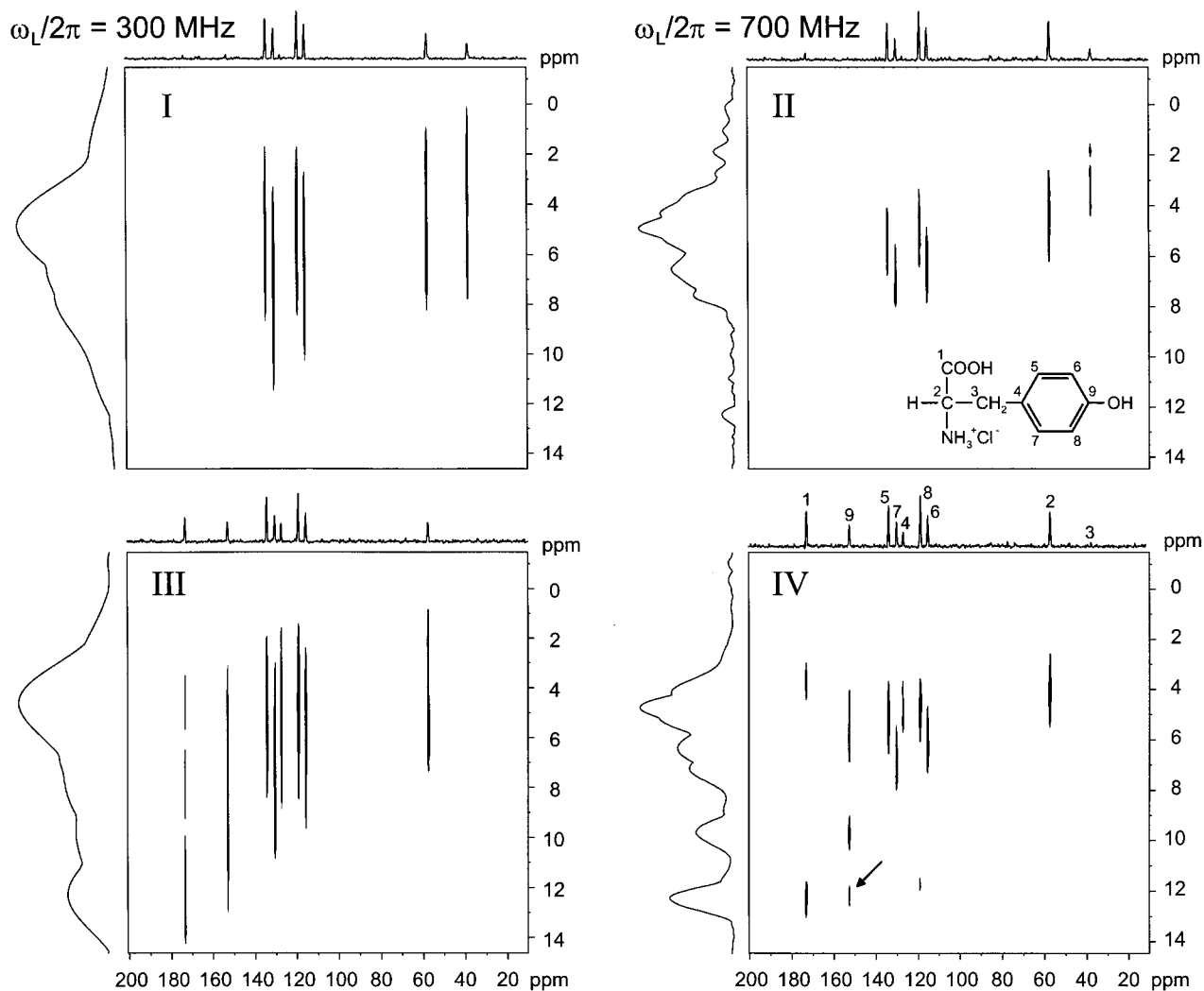


FIG. 2. REPT-HMQC spectra of L-tyrosine · HCl at 30 kHz MAS and magnetic field strengths corresponding to proton Larmor frequencies of 300 (I,III) and 700 MHz (II,IV), rotor-synchronized in t_1 . The MQ recoupling times were $1 \tau_R$ for spectra I and II, and $2 \tau_R$ for spectra III and IV, respectively. For each spectrum, skyline projections along both the MQ (^1H) and the ^{13}C dimensions are shown. The ^{13}C spectral assignments, denoted in IV, are according to Lesage *et al.* (9). The 300 MHz spectra were measured on a Bruker DSC 300 spectrometer equipped with a 2.5 mm MAS double-resonance probe using naturally abundant L-tyrosine · HCl, acquiring 32 slices in t_1 with 512 transients each (acquisition time approx. 5 h). The spectra at 700 MHz were measured on an only recently developed Bruker DRX 700 spectrometer using a narrow-bore magnet with 2.5 mm MAS equipment under the same conditions. The 90° pulse lengths were $2 \mu\text{s}$ on both channels; TPPM dipolar decoupling (28) with a proton B_1 field of 125 kHz was applied during acquisition. Contour levels start at about 20% of the maximum signal.

ance of the methylene (C_3) signal at longer recoupling times (Fig. 2, spectra III and IV). An effect common to all MQ methods is the relaxation of the MQ coherences during the excitation and reconversion intervals. It is here due to the influence of remote protons on the 2-spin coherences. The effect is most pronounced for moieties like methylene groups where, first, still a rather large perturbing homonuclear coupling among the two protons exists (which is only partially averaged out even at ultrafast MAS rates) and, second, the perturbing heteronuclear dipolar interaction of the additional proton on the carbon is just as large as the one-bond hetero-

nuclear coupling to be measured. This becomes even clearer when MQ spinning sidebands are recorded.

Figure 3 shows REPT-HMQC spectra recorded on the DSX 300 spectrometer using naturally abundant L-tyrosine · HCl, the basic difference to the spectra I and III in Fig. 2 only being that the t_1 increment is not set to a full rotor period but rather to a small value, such that the full spinning sideband patterns are recorded. Spectrum I, which was acquired with $1 \tau_R$ recoupling time, is dominated by first order spinning sidebands, the most intense signals being those of the carbons directly bound to protons. Spectrum II shows the corresponding MQ spinning

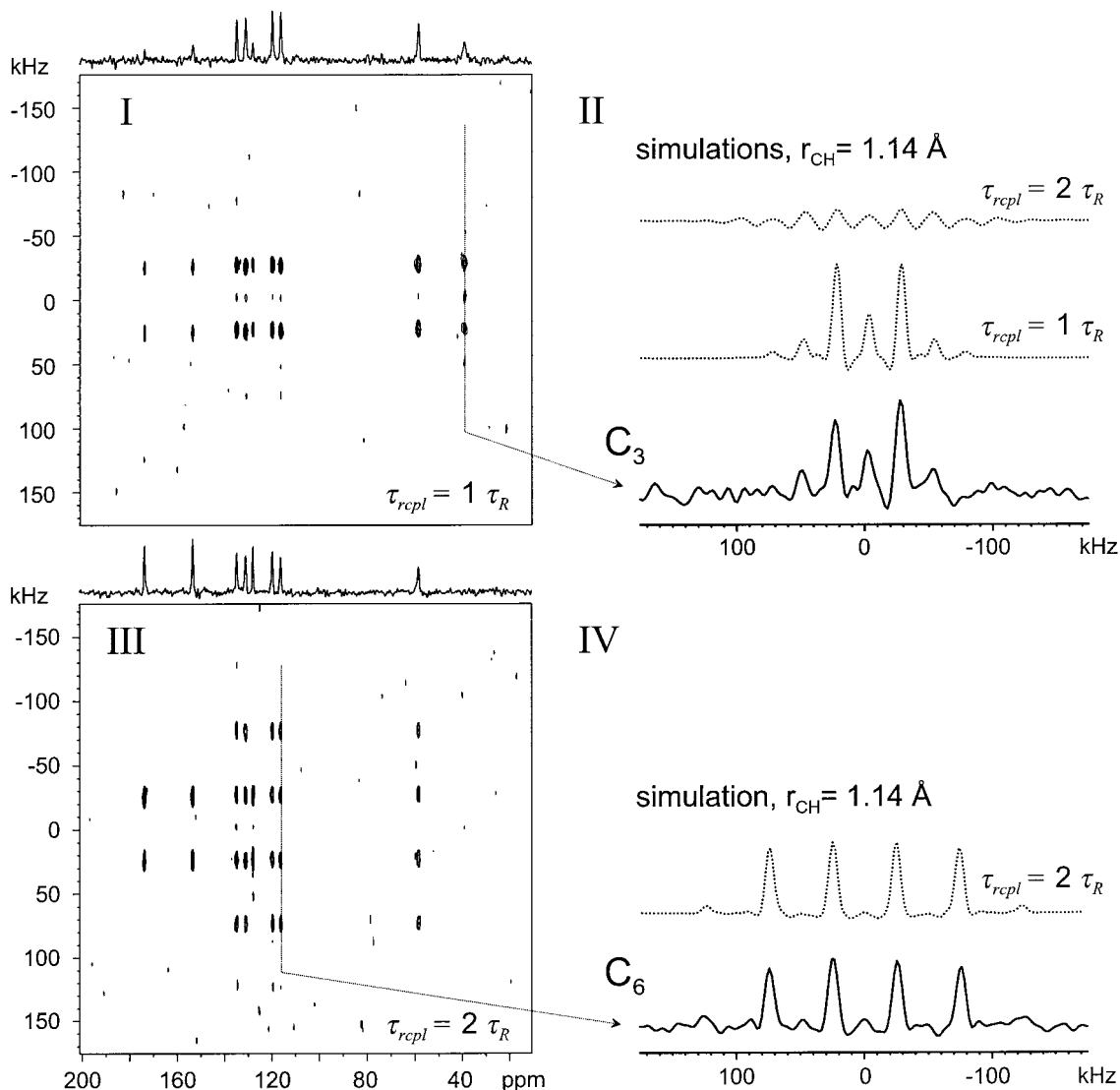


FIG. 3. REPT-HMQC spectra of *L*-tyrosine · HCl at 25 kHz MAS and a proton frequency of 300 MHz. MQ recoupling times were $1 \tau_R$ for spectrum I and $2 \tau_R$ for spectrum III. Due to a short t_1 increment of $2 \cdot 0.5 \mu\text{s}$ (corresponding to a spectral width of 500 kHz) the spectra exhibit spinning sideband patterns in the multiple-quantum dimension. Here, the projections shown on top of the spectra are the Fourier transforms of the first slices of the 2D data set, corresponding to HMQ-filtered spectra. Due to a weaker proton decoupling field of 83.3 kHz as compared to the spectra in Fig. 1, the aliphatic carbon signals are slightly broadened. Spectra II and IV represent sum projections along the direct dimensions of the methylene and the aromatic C_6 carbon signals, respectively, along with numerical density matrix simulations (dotted traces) for three spins assuming C–H distances of 1.14 Å. Finite pulse lengths were taken into account; for the methylene group, $r_{HH} = 1.8 \text{ \AA}$, and for the case of the aromatic C_6 –H group, the closest remote proton (C_5 –H) with $r_{HH} = 2.6 \text{ \AA}$, using the appropriate geometry, was included in the simulation. The simulated spectra in II are plotted on the same vertical scale, contour levels in spectra I and III start at about 5% of the maximum signal.

sideband pattern of the methylene group. Here, strong centerband and even order sideband intensity is observed, which cannot be explained from theory considering only a simple spin pair (Eqs. [5], [6]). As noted above, the methylene group is in some way a “pathological” case, in the sense that the strong perturbations (homo- and heteronuclear) imposed by the second proton lead to a considerable dephasing of the heteronuclear 2-spin mode during excitation and reconversion after only $2 \tau_R$. This is clearly demonstrated by the numerical simulations of the methylene group signals for 1 and $2 \tau_R$, thus

explaining the disappearance of the methylene signal in spectrum III. It should be mentioned that this restriction does not apply to methyl groups, since these are usually rapidly rotating, thus behaving inhomogeneously like a 2-spin system.

As expected, the spinning sideband patterns of the C–H moieties in the molecule look alike because the C–H bond lengths are similar for all C–H groups. As an example, spectrum IV in Fig. 3 shows the pattern for the aromatic C_6 carbon, along with a numerical simulation taking the closest remote proton into account. Again, weak centerband and even order

sideband intensity can be observed. As shown in [6], this is on the one hand due to the perturbing influence of remote protons and, on the other hand, to the contribution of CSA during the evolution in t_1 . It should be noted that the intensities of the odd order sidebands are hardly affected by the remote proton perturbation, so that an interpretation of the pattern using the expressions for a spin pair (Eqs. [5] and [6]) is possible. For a spectrum recorded on a 300 MHz spectrometer at 25 kHz MAS, modulations of the pattern due to CSA are negligibly small. At higher magnetic field strengths, though, pronounced distortions of the patterns occur for carbons with high CSAs. An approach showing how this problem can be circumvented will be presented in a further publication. Slight phase distortions in the spectra are in part due to finite pulse lengths, which have been taken into account in the simulations. From the simulation, we obtain a C–H bond length of the aromatic carbon of 1.14 Å, which compares well with the value $r_{CH} = 1.09$ Å from neutron diffraction studies (24). The difference of about 5% between distances from NMR measurements and distances from diffraction data has been observed before and can be explained by different averaging of fast vibrational motions (25). We note that the relative intensities of the different sideband orders is very sensitive to changes in the internuclear distance at the specified spinning speed and recoupling time, such that differences in distances of ± 0.03 Å can be discriminated.

We thus conclude that REPT-HMQC represents a promising new tool for advanced structure elucidation in solids. High proton resolution for ^{13}C – ^1H correlation is provided by high magnetic fields and ultra-fast MAS with spinning frequencies greater than 25 kHz. At such high spinning frequencies, heteronuclear dipolar coupling constants in situations where a carbon atom experiences one primary coupling to a proton can be measured virtually unperturbed by couplings to more remote protons. As a specific example, site-selective π -packing effects are detected. The pulse sequence is rather robust with respect to deviations from the ideal 90° and 180° pulse lengths, on precise rotor synchronization, spectral offsets on both channels, and S spin CSA. The experiment may not only be valuable for the application to spectral assignment and structure refinement problems, it has already proven to be useful for ^{13}C site-resolved studies of the dynamics of complex organic molecules in the solid state by analyzing motional averaging of dipolar couplings. These results, along with a more quantitative treatment of the theoretical capabilities and limitations of the technique, are currently being prepared for publication.

ACKNOWLEDGMENTS

The authors thank Steven P. Brown, Claudiu Filip, and Klaus Schmidt-Rohr for stimulating discussions. Financial support was provided by the Deutsche Forschungsgemeinschaft, SFB 262.

REFERENCES

1. J. Gottwald, D. E. Demco, R. Graf, and H. W. Spiess, *Chem. Phys. Lett.* **243**, 314–323 (1995).
2. K. Schmidt-Rohr, *Macromolecules* **29**, 3975–3981 (1996).
3. X. Feng, P. J. E. Verdegem, Y. K. Lee, D. Sandström, M. Edén, P. Bovee-Geurts, W. J. de Grip, J. Lugtenburg, H. J. M. de Groot, and M. H. Levitt, *J. Am. Chem. Soc.* **119**, 6853–6857 (1997).
4. I. Schnell, S. P. Brown, H. Y. Lew, H. Ishida, and H. W. Spiess, *J. Am. Chem. Soc.* **120**, 11784–11795 (1998).
5. W. Sommer, J. Gottwald, D. E. Demco, and H. W. Spiess, *J. Magn. Reson.* **A 113**, 131–134 (1995).
6. K. Saalwächter, R. Graf, D. E. Demco, and H. W. Spiess, *J. Magn. Reson.* **139**, 287–301 (1999).
7. K. Schmidt-Rohr, J. Clauss, and H. W. Spiess, *Macromolecules* **25**, 3273–3277 (1992).
8. A. Lesage, S. Steuernagel, and L. Emsley, *J. Am. Chem. Soc.* **120**, 7095–7100 (1998).
9. A. Lesage, D. Sakellariou, S. Steuernagel, and L. Emsley, *J. Am. Chem. Soc.* **120**, 13194–13201 (1998).
10. B.-J. van Rossum, G. J. Boender, and H. J. M. de Groot, *J. Magn. Reson. A* **120**, 274–277 (1996).
11. C. Filip, S. Hafner, I. Schnell, D. E. Demco, and H. W. Spiess, *J. Chem. Phys.* **110**, 423–440 (1999).
12. L. Müller, *J. Am. Chem. Soc.* **101**, 4481–4484 (1979).
13. A. Bax, R. H. Griffey, and B. L. Hawkins, *J. Magn. Reson.* **55**, 301–315 (1983).
14. T. Gullion and J. Schaefer, *J. Magn. Reson.* **81**, 196–200 (1989).
15. T. Gullion and J. Schaefer, *Adv. Magn. Reson.* **13**, 57–83 (1989).
16. T. Gullion, *Magn. Reson. Rev.* **17**, 83–131 (1997).
17. M. Hong, J. D. Gross, R. G. Griffin, *J. Phys. Chem. B* **101**, 5869–5874 (1997).
18. O. W. Sørensen, G. W. Eich, M. H. Levitt, G. Bodenhausen, and R. R. Ernst, *Progr. NMR Spectrosc.* **16**, 163–192 (1983).
19. H. Geen, J. J. Titman, J. Gottwald, and H. W. Spiess, *J. Magn. Reson. A* **114**, 264–267 (1995).
20. B.-J. van Rossum, H. Förster, and H. J. M. de Groot, *J. Magn. Reson.* **124**, 516–519 (1997).
21. S. Hafner and H. W. Spiess, *J. Magn. Reson. A* **121**, 160–166 (1996).
22. I. Schnell, A. Lupulescu, S. Hafner, D. E. Demco, and H. W. Spiess, *J. Magn. Reson.* **133**, 61–69 (1998).
23. S. B. Brown, I. Schnell, J. D. Brand, K. Müllen, and H. W. Spiess, *J. Am. Chem. Soc.* **121**, 6712–6718 (1999).
24. M. N. Frey, T. F. Koetzle, M. S. Lehmann, and W. C. Hamilton, *J. Chem. Phys.* **58**, 2547–2556 (1973).
25. T. Nakai, J. Ashida, and T. Terao, *Mol. Phys.* **67**, 839–847 (1989).
26. T. Gullion, D. B. Baker, and M. S. Conradi, *J. Magn. Reson.* **89**, 479–484 (1990).
27. K. Schmidt-Rohr and H. W. Spiess, "Multidimensional Solid-State NMR and Polymers," Academic Press, San Diego (1997).
28. A. E. Bennet, C. M. Rienstra, M. Auger, K. V. Lakshmi, and R. G. Griffin, *J. Chem. Phys.* **103**, 6951–6958 (1995).